Article

Turn-On Fluorescence Sensing of Nucleoside Polyphosphates Using a Xanthene-Based Zn(II) Complex Chemosensor

Akio Ojida, Ippei Takashima, Takahiro Kohira, Hiroshi Nonaka, and Itaru Hamachi

J. Am. Chem. Soc., **2008**, 130 (36), 12095-12101 • DOI: 10.1021/ja803262w • Publication Date (Web): 14 August 2008

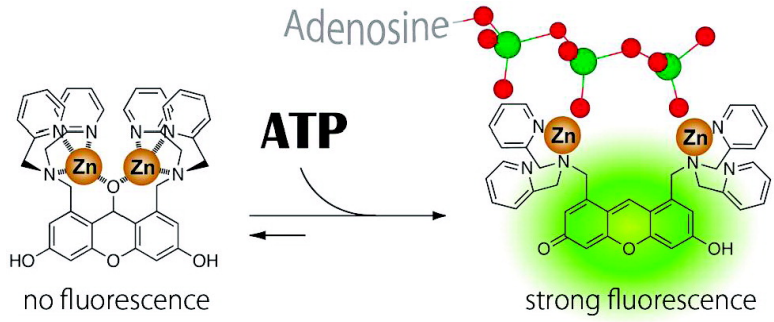

More About This Article

Additional resources and features associated with this article are available within the HTML version:

- Supporting Information
- Links to the 1 articles that cite this article, as of the time of this article download
- Access to high resolution figures
- Links to articles and content related to this article
- Copyright permission to reproduce figures and/or text from this article

View the Full Text HTML

J|A|C|S
ARTICLES

Published on Web 08/14/2008

Turn-On Fluorescence Sensing of Nucleoside Polyphosphates Using a Xanthene-Based Zn(II) Complex Chemosensor

Akio Ojida, Ippei Takashima, Takahiro Kohira, Hiroshi Nonaka, and Itaru Hamachi*

Department of Synthetic Chemistry and Biological Chemistry, Graduate School of Engineering, Kyoto University, Katsura Campus, Nishikyo-ku, Kyoto, 615-8510, Japan and PRESTO (Life Phenomena and Measurement Analysis, JST), Sanbancho, Chiyoda-ku, Tokyo, 332-0012, Japan

Received May 2, 2008; E-mail: ihamachi@sbchem.kyoto-u.a.jp

Abstract: Fluorescence sensing with small molecular chemosensors is a versatile technique for elucidation of function of various biological substances. We now report a new fluorescent chemosensor for nucleoside polyphosphates such as ATP using metal−anion coordination chemistry. The chemosensor **1**−2Zn(II) is comprised of the two sites of 2,2′-dipicolylamine (Dpa)−Zn(II) as the binding motifs and xanthene as a fluorescent sensing unit for nucleoside polyphosphates. The chemosensor **1**−2Zn(II) selectively senses nucleoside polyphosphates with a large fluorescence enhancement ($F/F_o > 15$) and strong binding affinity ($K_{app} \approx 1 \times 10^6\ M^{-1}$), whereas no detectable fluorescence change was induced by monophosphate species and various other anions. The 'turn-on,' fluorescence of **1**−2Zn(II) is based on a new mechanism, which involves the binding-induced recovery of the conjugated form of the xanthene ring from its nonfluorescent deconjugated state which was formed by an unprecedented nucleophilic attack of zinc-bound water. The selective and highly sensitive ability of **1**−2Zn(II) to detect nucleoside polyphosphates enables its bioanalytical applications in fluorescence visualization of ATP particulate stores in living cells, demonstrating the potential utility of **1**−2Zn(II).

Introduction

Fluorescence measurement of specific biological molecules by artificial chemosensors is a versatile technique with high sensitivity, rapid response, and easy performance, offering utility not only for in vitro assays but also for in vivo imaging studies using fluorescence microscopy.[1] During the past few decades, much effort has been devoted to the development of fluorescent chemosensors for various biological substances such as cations, anions, sugars, and proteins. Significant progress has been made in the measurement of cations. In fact, based on a comprehensive knowledge of coordination chemistry, a number of practically useful sensors for Ca^{2+}, Zn^{2+}, Mg^{2+}, etc., have been designed, some of which are now available for imaging studies in living cells and contribute to understanding the physiological roles of cations.[2] In contrast, fluorescent chemosensors for biologically relevant anions have remained a challenging topic. This is mainly due to the difficulty of design of a binding motif for anionic species that works well in aqueous solution. In addition, there has been no general design principle for the effective transduction of an anion-binding event to a large fluorescent signal change.[3]

Nucleoside polyphosphates play pivotal roles in various physiological events, for example, it is well known that ATP is a universal energy source for various cellular functions in all living systems. Nucleoside polyphosphates are also involved in many enzymatic processes as reactive substrates. For example, ATP serves as a phosphate donor in kinase-catalyzed protein phosphorylation, and UDP-glycosides are used as substrates in many glycosylation processes catalyzed by glycosyltransferases. In addition to these fundamental intracellular roles, nucleoside polyphosphates such as ATP, ADP, and a variety of diadenosine polyphosphates also play important extracellular roles as signaling substances.[4] Therefore, much effort has been devoted to the development of luminescent detection systems for these nucleoside polyphosphates.[5] Several fluorescent chemosensors have been reported in recent decades,[6] but only a few of them have a strong binding affinity and a large fluorescence response to a target nucleoside polyphosphate in aqueous solution. Consequently, the bioanalytical application of these chemosensors for in vitro and in vivo sensing is still very limited.[6b,c,i,7]

We recently reported a binuclear 2,2′-dipicolylamine (Dpa)−zinc(II) complex as a useful binding motif for phosphate anion

(1) (a) Geddes, C. D.; Lakowicz, J. R. *Topics in Fluorescence Spectroscopy*; Springer: New York, 2005; Vol. 9. (b) Geddes, C. D.; Lakowicz, J. R. *Topics in Fluorescence Spectroscopy*; Springer: New York, 2005; Vol. 10.

(2) (a) Haugland, R. P. *Guide to Fluorescent Probes and Labeling Techniques*; Invitrogen: USA, 2005; Chapter 19. (b) Domaille, D. W.; Que, E. L.; Chang, C. J. *Nat. Chem. Biol.* **2008**, *4*, 168. (c) Kikuchi, K.; Komatsu, K.; Nagano, T. *Curr. Opin. Chem. Biol.* **2004**, *8*, 182. (d) Grynkiewwicz, G.; Poenie, M.; Tsien, R. Y. *J. Biol. Chem.* **1985**, *260*, 3440.

(3) (a) O'Neil, E. J.; Smith, B. D. *Coord. Chem. Rev.* **2006**, *250*, 3068. (b) Martínez-Máñez, R.; Sancenón, F. *Chem. Rev.* **2003**, *103*, 4419. (c) Beer, P. D.; Gale, P. A. *Angew. Chem., Int. Ed.* **2001**, *40*, 486.

(4) (a) Burnstock, G. *Pharmacol. Rev.* **2006**, *58*, 58. (b) Bodin, P.; Burnstock, G. *Neurochem. Res.* **2001**, *26*, 959. (c) Chen, Y.; Corriden, R.; Inoue, Y.; Yip, L.; Hashiguchi, N.; Zinkernagel, A.; Nizet, V.; Insel, P. A.; Junger, W. G. *Science* **2006**, *314*, 1792. (d) Gourine, A. V.; Llaudet, E.; Dale, N.; Spyer, M. *Nature* **2005**, *436*, 108.

(5) (a) Willemse, W.; Janssen, E.; de Lange, F.; Wieringa, B.; Fransen, J. *Nat. Biotechnol.* **2007**, *25*, 170. (b) Corriden, R.; Insel, P. A.; Junger, W. G. *Am. J. Physiol. Cell Physiol.* **2007**, *293*, C1420. (c) Nakamura, M.; Mie, M.; Funabashi, H.; Yamamoto, K.; Ando, J.; Kobatake, E. *Anal. Biochem.* **2006**, *352*, 61. (d) Pellegatti, P.; Falzoni, S.; Pinton, P.; Rizzuto, R.; Di Virgilio, F. *Mol. Biol. Cell* **2005**, *16*, 3659.

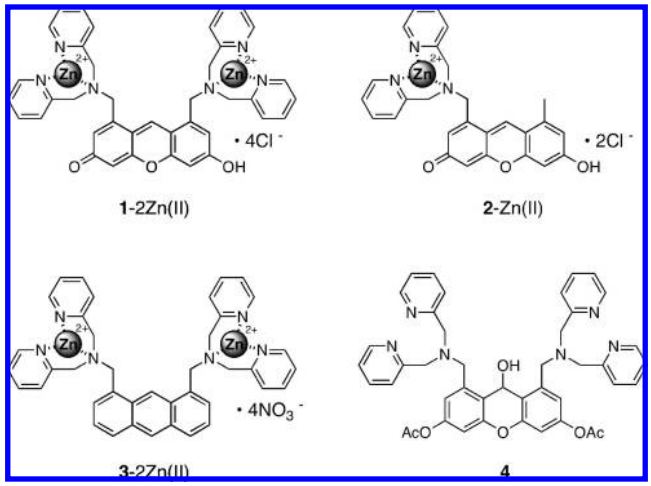

and developed several fluorescent chemosensors such as the anthracene derivative **3**−2Zn(II) for detection of biologically relevant phosphate derivatives.[8] Although they bind strongly to nucleoside polyphosphates and fluorescently sense them under neutral aqueous conditions, their utility in bioanalytical applications has been limited in in vitro applications such as enzyme activity assays.[9] This limitation is due mainly to their small emission or excitation change and short excitation wavelength (<450 nm) as well as their moderate sensing selectivity among phosphate derivatives. Here we describe new binuclear zinc complex **1**−2Zn(II) with a xanthene fluorophore that serves as a selective chemosensor for nucleoside polyphosphates. **1**−2Zn(II) shows a remarkably large fluorescence enhancement upon binding to a nucleoside polyphosphate such as ATP under neutral aqueous conditions. We demonstrated that the off/on fluorescence sensing of **1**−2Zn(II) is based on a new mechanism, which involves the binding-induced recovery of the fluorescent xanthene ring from an unprecedented unique non-

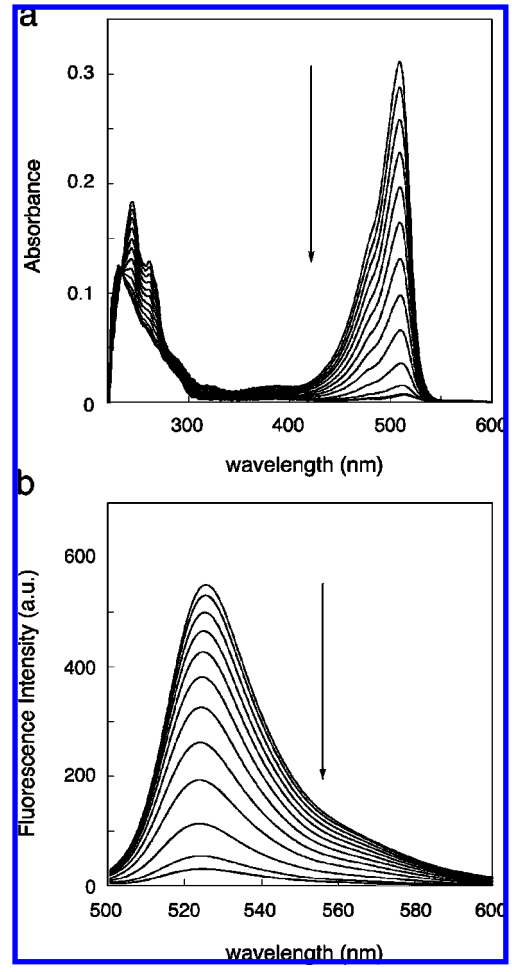

Figure 1. UV absorption (a) and fluorescence (b) spectral change of the ligand **1** upon addition of $ZnCl_2$ (0−15 μM). Measurement conditions: 5 μM **1** in 50 mM HEPES, 10 mM NaCl, 1 mM $MgCl_2$ (pH 7.4)−MeOH (1:1), 25 °C, λ_{ex} = 488 nm in b.

fluorescent form. Taking advantage of the off/on fluorescence sensing specifically of polyphosphate by **1**−2Zn(II), this chemosensor was successfully applied to fluorescence imaging studies of intracellular ATP stores in living cells.

Results and Discussion

Synthesis of **1**−2Zn(II) is outlined in Scheme 1. Compound **5**[8b] was converted to **7** by radical bromination with NBS, followed by nucleophilic substitution with 2,2′-dipicolylamine (Dpa) at both methyl groups. Reduction of the ketone group of **7** with $LiBH_4$/TMSCl and subsequent oxidization with DDQ yielded ligand **1**,[10] which was complexed with 2 equiv of $ZnCl_2$ to give the zinc(II) complex **1**−2Zn(II). According to a similar synthetic procedure, the mononuclear zinc(II) complex **2**−Zn(II) was prepared from the monobromo derivative of **6** (Scheme S1).

The zinc(II) complex **1**−2Zn(II) unexpectedly showed a weak fluorescence emission ($\lambda_{em,max}$ = 522 nm) and small UV absorption at 509 nm (ϵ = 2800 $M^{-1}\cdot cm^{-1}$) in neutral aqueous conditions (50 mM HEPES, pH 7.4). These spectroscopic properties are in sharp contrast to those of ligand **1**, which exhibited a strong fluorescence emission and large UV absorption at 509 nm (ϵ = 65 000 $M^{-1}\cdot cm^{-1}$) in aqueous MeOH

(6) (a) Aoki, S.; Kimura, E. *Rev. Mol. Biotechnol.* **2002**, *90*, 129. (b) Schäferling, M.; Wolfbeis, O. S. *Chem. Eur. J.* **2007**, *13*, 4342. (c) Rhee, H.-W.; Choi, H.-Y.; Han, K.; Hong, J.-I. *J. Am. Chem. Soc.* **2007**, *129*, 4524. (d) Neelakandan, P. P.; Hariharan, M.; Ramaiah, D. *J. Am. Chem. Soc.* **2006**, *128*, 11334. (e) Kwon, J. Y.; Singh, N. J.; Kim, H. N.; Kim, S. K.; Kim, K. S.; Yoon, J. *J. Am. Chem. Soc.* **2004**, *126*, 8892. (f) Abe, H.; Mawatari, Y.; Teraoka, H.; Fuijimoto, K.; Inouye, M. *J. Org. Chem.* **2004**, *69*, 495–504. (g) Lee, D. H.; Kim, S. Y.; Hong, J.-I. *Angew. Chem., Int. Ed.* **2004**, *43*, 4777. (h) Fabbrizzi, L.; Marcotte, N.; Stomeo, F.; Taglietti, A. *Angew. Chem., Int. Ed.* **2002**, *41*, 3811. (i) Mizukami, S.; Nagano, T.; Urano, Y.; Odani, A.; Kikuchi, K. *J. Am. Chem. Soc.* **2002**, *124*, 3920. (j) Sancenón, F.; Descalzo, A. B.; Martínez-Máñez, R.; Miranda, M. A.; Soto, J. *Angew. Chem., Int. Ed.* **2001**, *40*, 2640. (k) Schneider, S. E.; O'Neil, S. N.; Anslyn, E. V. *J. Am. Chem. Soc.* **2000**, *122*, 542. (l) Hosseini, M. W.; Blacker, A. J.; Lehn, J.-M. *J. Am. Chem. Soc.* **1990**, *112*, 3896.
(7) Leevy, W. M.; Gammon, S. T.; Jiang, H.; Johnsson, J. R.; Maxwell, D. J.; Jackson, E. N.; Marquez, M.; Piwnica-Worms, D.; Smith, B. D. *J. Am. Chem. Soc.* **2006**, *128*, 16476.
(8) (a) Ojida, A.; Hamachi, I. *Bull. Chem. Soc. Jpn.* **2006**, *79*, 35. (b) Ojida, A.; Nonaka, H.; Miyahara, Y.; Tamaru, S.; Sada, K.; Hamachi, I. *Angew. Chem., Int. Ed.* **2006**, *45*, 5518. (c) Ojida, A.; Miyahara, Y.; Wongkongkatep, J.; Tamaru, S.; Sada, K.; Hamachi, I. *Chem. Asian J.* **2006**, *1*, 555. (d) Ojida, A.; Inoue, M.; Mito-oka, Y.; Tsutsumi, H.; Sada, K.; Hamachi, I. *J. Am. Chem. Soc.* **2006**, *128*, 2052. (e) Ojida, A.; Mito-oka, Y.; Sada, K.; Hamachi, I. *J. Am. Chem. Soc.* **2004**, *126*, 2454. (f) Ojida, A.; Inoue, M.; Mito-oka, Y.; Hamachi, I. A. *J. Am. Chem. Soc.* **2003**, *125*, 10184. (g) Ojida, A.; Park, S.-K.; Mito-oka, Y.; Hamachi, I. *Tetrahedron Lett.* **2002**, *43*, 6193. (h) Ojida, A.; Mito-oka, Y.; Inoue, M.; Hamachi, I. *J. Am. Chem. Soc.* **2002**, *124*, 6256.
(9) (a) Wongkongkatep, J.; Miyahara, Y.; Ojida, A.; Hamachi, I. *Angew. Chem., Int. Ed.* **2006**, *118*, 665. (b) Ojida, A.; Kohira, T.; Hamachi, I. *Chem. Lett.* **2004**, *33*, 1024.
(10) Shi, J.; Zhang, X.; Neckers, D. C. *J. Org. Chem.* **1992**, *57*, 4418.

Scheme 1. Synthesis of the Chemosensor **1**−2Zn(II)

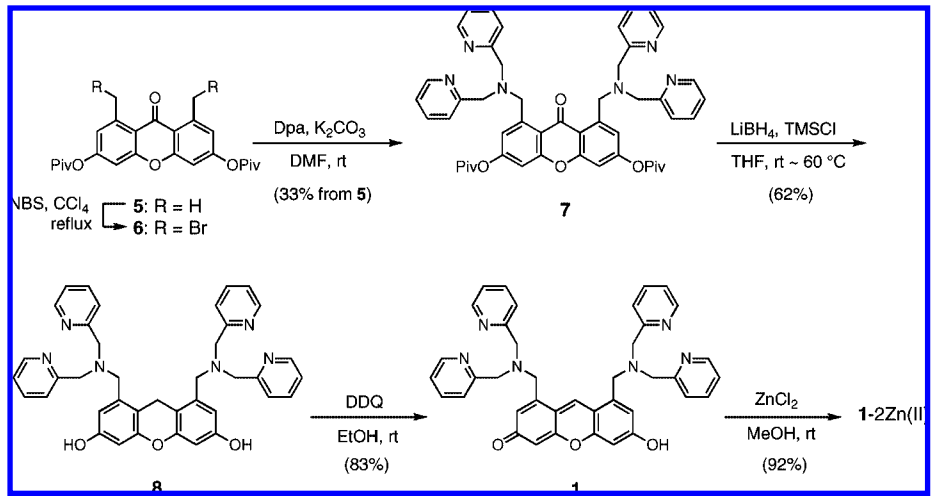

Scheme 2. Structural Equilibrium of **1**−2Zn(II) under Neutral Aqueous Conditions

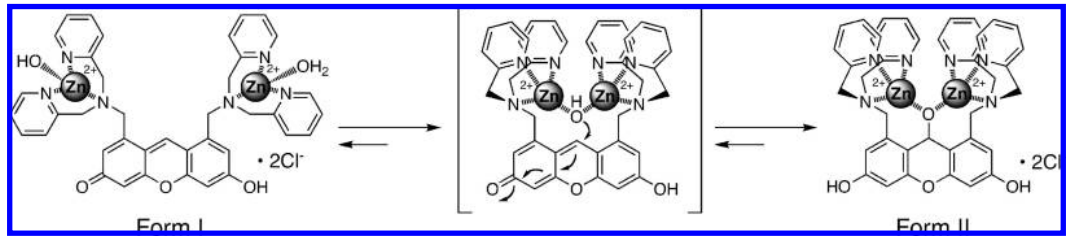

solution (50 mM HEPES (pH 7.4):MeOH = 1:1). On titration of ligand **1** with $ZnCl_2$, the absorbance at 509 nm gradually decreased and almost completely disappeared upon addition of 2 equiv of $ZnCl_2$ accompanied by a marked decrease of the fluorescence emission (Figure S1, Supporting Information). These spectral changes suggested that Zn(II) coordination to the Dpa sites of **1** caused destruction of the conjugated structure of the xanthene fluorophore. The X-ray crystallographic analysis of **1**−2Zn(II) revealed that deconjugation of the xanthene ring is induced by nucleophilic attack of the water molecule coordinated to the two zinc(II) ions (Figure 2). Crystallization of **1**−2Zn(II)·$4ClO_4^-$ from MeOH−H_2O under the conditions of careful pH adjustment (pH 7.5) gave colorless prisms suitable for X-ray crystallography. The complex has the binuclear zinc(II) core bridged by oxygen atom O(4) derived from a Zn(II)-bound water molecule.[11] Interestingly, the μ-oxygen O(4) also forms a O−C bond with the C(9) carbon of the xanthene ring (O(4)−C(9) = 1.454 Å) by which the conjugated structure of the xanthene was destroyed. The deconjugated form of **1**−2Zn(II) was also confirmed by high-resolution FAB mass spectroscopy. The neutral aqueous solution (pH 7.4) of **1**−2Zn(II))$4Cl^-$ gave the parent peak at 849.0714, which can be assigned as the form II complex $[\mathbf{1}-2Zn(II)(O)(Cl)_2]^+$ (exact mass 849.0680) having a μ-oxygen atom bridging the two zinc(II) ions (Scheme 2). On the other hand, a slightly acidic solution (pH 4−5) of **1**−2Zn(II)·$4Cl^-$ gave the parent peak at 867.0790, which can be assigned as the conjugated form I ($[\mathbf{1}-2Zn(II)(Cl)_2(OH)(H_2O)]^+$, exact mass 867.0785) having the two coordinated water molecules instead of the μ-oxygen atom. These results showed that there is an equilibrium between the two forms in aqueous solution depending on pH and that **1**−2Zn(II) exists predominantly as the deconjugated form II under neutral aqueous conditions (Scheme 2). In contrast, in the case of the mononuclear complex **2**−Zn(II), the zinc(II) coordination to the Dpa site induced neither an absorption decrease (λ_{max} = 507 nm) nor an emission decrease (λ_{max} = 523 nm) (Figure S2). It is clear that no structural change of the xanthene ring was induced by the mononuclear coordination of zinc(II), implying that the bridging water molecule between the two zinc(II) centers in **1**−2Zn(II) is essential to induce nucleophilic attack to the xanthene ring in neutral pH.

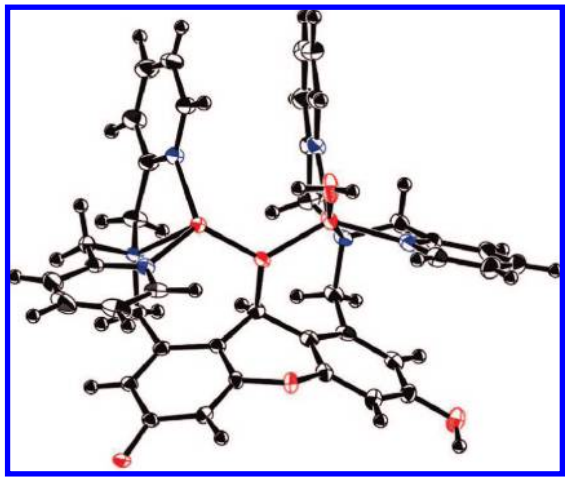

Figure 2. ORTEP diagrams (50% probability ellipsoids) of **1**−2Zn(II) ($C_{39}H_{34}N_6O_4Zn_2 \cdot 2ClO_4 \cdot 3H_2O$). The perchlorate anions and noncoordinated water molecules are omitted for clarity.

(11) (a) Reports of the μ-oxo−dizinc structure in natural enzymes and artificial enzyme mimics: Matsufuji, K.; Shiraishi, H.; Miyasato, Y.; Shiga, T.; Ohba, M.; Yokoyama, T.; Okawa, H. *Bull. Chem. Soc. Jpn.* **2005**, *78*, 851. (b) He, C.; Lippard, S. J. *J. Am. Chem. Soc.* **2000**, *122*, 184. (c) Lipscomb, W. N.; Sträter, N. *Chem. Rev.* **1996**, *96*, 2375.

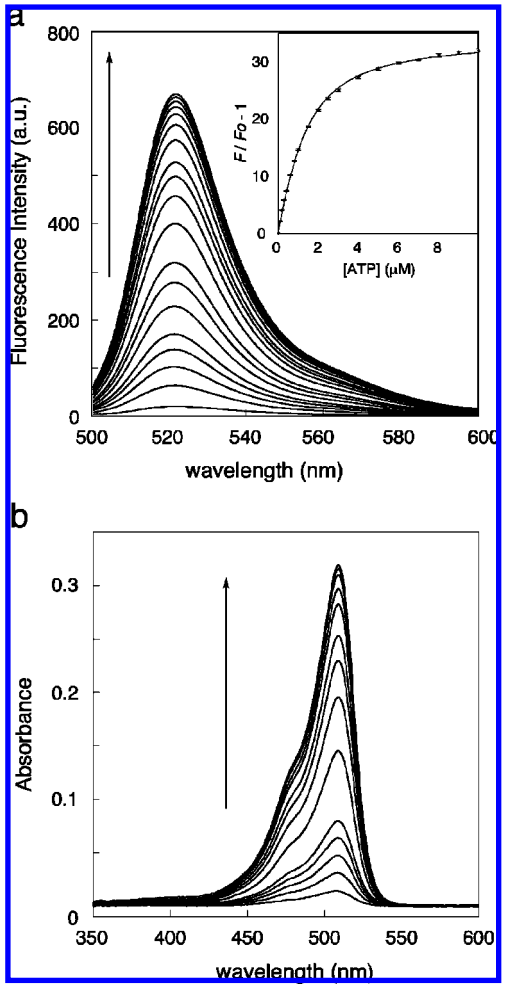

Figure 3. Titration profiles of **1**−2Zn(II) upon addition of ATP (0−10 μM). (a, b) Fluorescence emission (a) and UV absorption (b) change of **1**−2Zn(II). (inset) Curve-fitting analysis of the fluorescence emission change at 523 nm. Measurement conditions: 1 (a) or 5 μM (b) **1**−2Zn(II) in 50 mM HEPES, 10 mM NaCl, 1 mM $MgCl_2$, pH 7.4, λ_{ex} = 488 nm, 25 °C.

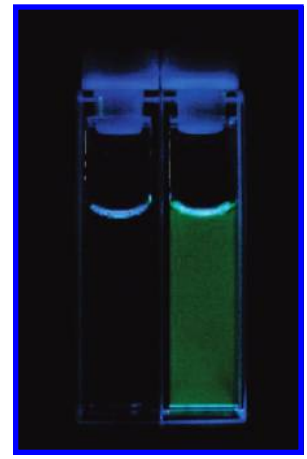

Figure 4. Photograph of the aqueous solution of **1**−2Zn(II) in the absence (left) and presence (right) of ATP (1 μM). Measurement conditions: 1 μM of **1**−2Zn(II) in 50 mM HEPES, pH 7.4, λ_{ex} = 365 nm, 25 °C.

Table 1. Summary of the Apparent Binding Constants (K_{app}, M^{-1}) of **1**−2Zn(II) to Various Anions and the Relative Emission Intensity (F/F_o) against the Initial State[a]

anion species[b]	K_{app} (M^{-1})	F/F_o[d]	anion species[b]	K_{app} (M^{-1})	F/F_o[d]
ATP	1.3×10^6	33	c-GMP	n.d.[c]	*e*
ADP	1.7×10^6	18	c-AMP	1.4×10^3	7[f]
AMP	n.d.[c]	*e*	ADP-Glu	n.d.[c]	*e*
GTP	1.7×10^6	34	UDP-Glu	n.d.[c]	*e*
CTP	6.8×10^5	31	AcO^-	n.d.[c]	*e*
UDP	4.9×10^5	20	SO_4^{2-}	n.d.[c]	*e*
PPi	4.0×10^7	55	NO_3^-	n.d.[c]	*e*
IP_3	3.3×10^6	27	HCO_3^-	n.d.[c]	*e*
HPO_4^{2-}	n.d.[c]	*e*			

[a] Measurement conditions: 1 μM **1**−2Zn(II) in 50 mM HEPES, 10 mM NaCl, 1 mM $MgCl_2$, pH 7.4, λ_{ex} = 488 nm, 25 °C. [b] The abbreviations of the anions are described in the Experimental Section. [c] Not determined due to the small fluorescence change. [d] Unless otherwise noted, F/F_o indicates the relative fluorescence intensity (F) at 523 nm of **1**−2Zn(II) in the presence of 10 μM of the anion against that of the initial state (F_o). [e] Negligible fluorescence change was observed even in the presence of 1 mM anion. [f] Relative fluorescence intensity of **1**−2Zn(II) in the presence of 1 mM of the cAMP.

A remarkably large fluorescence enhancement was observed as shown in Figure 3a, when ATP was added to the neutral aqueous solution of **1**−2Zn(II) (1 μM of **1**−2Zn(II) in 50 mM HEPES, 10 mM NaCl, 1 mM $MgCl_2$, pH 7.4). The fluorescence intensity at 523 nm increased by more than 30-fold upon addition of 10 μM ATP, and the plot of the fluorescence intensity change ($F/F_o - 1$) showed typical saturation behavior. Curve-fitting analysis gave the affinity constant (K_{app}, M^{-1}) of 1.3×10^6 M^{-1} for ATP. The fluorescence Job's plot conducted between **1**−2Zn(II) and ATP unequivocally determined that the binding stoichiometry is 1:1 (Figure S3). The fluorescence quantum yield of the binding complex of **1**−2Zn(II) with ATP is sufficiently high (Φ = 0.61). A photograph of the turn-on fluorescence of **1**−2Zn(II) upon binding to ATP clearly demonstrated the naked eye detection of ATP using **1**−2Zn(II) (Figure 4). These superior properties of **1**−2Zn(II) as a fluorescent chemosensor allowed us to sense less than 10^{-6} M ATP with a sufficient fluorescence intensity and high signal/noise ratio.

The sensing selectivity of **1**−2Zn(II) for a variety of biologically relevant anions was evaluated by fluorescence titration experiments. Table 1 summarizes the affinity constant (K_{app}, M^{-1}) and emission increase ratio (F/F_o at 523 nm) obtained under the neutral aqueous conditions (1 μM of **1**−2Zn(II) in 50 mM HEPES buffer, 10 mM NaCl, 1 mM $MgCl_2$, pH 7.4). The chemosensor **1**−2Zn(II) showed a strong binding affinity (K_{app}, M^{-1}) in the range from 4.9×10^5 to 1.7×10^6 M^{-1} toward various polyphosphate derivatives such as XTP (X = A, G, C) and XDP (X = A, U). The stronger binding affinities were obtained for pyrophosphate (PPi) and inositol-1,3,4-trisphosphate (IP_3), probably due to their highly negative characters suitable for binding with the cationic **1**−2Zn(II). The chemosensor **1**−2Zn(II) showed a large fluorescence enhancement toward polyphosphate derivatives such as XTP (X = A, G, C, F/F_o > 30), XDP (X = A, U, F/F_o > 15), and pyrophosphate ($P_2O_7^{4-}$, F/F_o = 54). On the other hand, the fluorescence change was not induced even by a high concentration (1 mM) of monophosphorylated species such as HPO_4^{2-}, AMP, cGMP, and phospho-diesters such as UDP-galactose or by other anions (SO_4^{2-}, NO_3^-, HCO_3^-, CH_3COO^-). These results suggest that **1**−2Zn(II) is a useful probe for the fluorescence detection of the polyphosphates with high selectivity and strong binding affinity, giving a good signal/noise ratio.

The turn-on fluorescence sensing of **1**−2Zn(II) for nucleoside polyphosphates can be ascribed to the recovery of the conjugated structure of the xanthene ring. As mentioned above, the

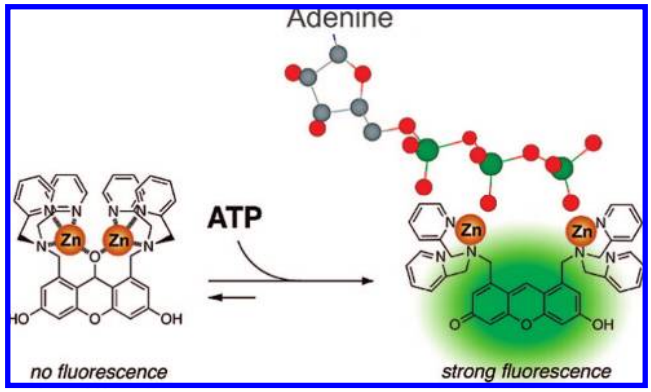

Figure 5. Schematic illustration of the turn-on fluorescence sensing mechanism of **1**−2Zn(II) for ATP.

fluorescence off state of **1**−2Zn(II) is due to formation of the deconjugated structure of the xanthene fluorophore. Although many fluorescein derivatives are known to form a deconjugated xanthene structure induced by intramolecular attack of the adjacent carboxylate anion group,[12] the present deconjugation involving nucleophilic attack of a metal-bound water molecule is the first example of this type to the best of our knowledge. As shown in Figure 3b, a very weak absorbance of **1**−2Zn(II) at 509 nm due to the conjugated xanthene ring increased continuously upon addition of ATP. Curve-fitting analysis of the UV titration curve afforded the affinity constant of $9.6 \times 10^5\ M^{-1}$ for ATP, in good agreement with the value determined by the fluorescence titration. Both the UV and fluorescence analyses indicate that ATP binding to the two Zn(II)−Dpa sites induces the disruption of the μ-oxo−dizinc(II) core of **1**−2Zn(II) due to the multipoint interactions between two Dpa−Zn(II) sites and the triphosphate group of ATP, which results in the recovery of the conjugated xanthene structure showing strong fluorescence emission, as schematically illustrated in Figure 5.[13] In the comparison with the fluorescence recovery, **1**−2Zn(II) showed a lower recovery ratio in the binding with ADP ($F/F_o = 18$) than ATP ($F/F_o = 33$), irrespective of the almost same binding affinity toward these polyphosphate species (Table 1). The UV titration experiments showed that the absorption recovery of **1**−2Zn(II) at 509 nm in the binding complex with ADP ($A/A_o = 13$) is also smaller than that with ATP ($A/A_o = 18$) (Figure S4), indicating that the fluorescence recovery ratio is partially attributable to the difference of their absorbance in the excitation wavelength region. No recovery of the emission and absorption of **1**−2Zn(II) was observed by addition of monophosphates and phosphodiesters (Table 1, Figure S4), suggesting that the multiple interactions with di- or triphosphate groups of the polyphosphates was essential to disrupt the μ-oxo−dizinc(II) core of **1**−2Zn(II).

Taking advantage of the selective sensing ability of **1**−2Zn(II) for the nucleoside polyphosphates, we applied **1**−2Zn(II) to the

(12) Haugland, R. P. *A Guide to Fluorescent Probes and Labeling Techniques*; Invitrogen: USA, 2005; Chapter 20.

(13) In the binding complex with the nucleoside triphosphate such as ATP, we propose that the β- and γ-phosphate groups interact with the two Zn(II)−Dpa sites of **1**−2Zn(II) as shown in Figure 5. This is speculated by a ^{31}P NMR study (0.5 mM in 50 mM HEPES, pH 7.4) in which the peaks corresponding to β- and γ-phosphate of ATP observed at −20.7 and −5.9 ppm are shifted downfield at −19.2 and −5.2 ppm, respectively, upon addition of 1 equiv of **1**−2 Zn(II) while the peak corresponding to the α-phosphate observed at −9.6 ppm only slightly shifted upfield at −9.9 ppm. Such a two-point binding mode involving the two phosphate groups may reasonably explain the strong binding affinity of **1**−2Zn(II) for the nucleoside polyphosphates.

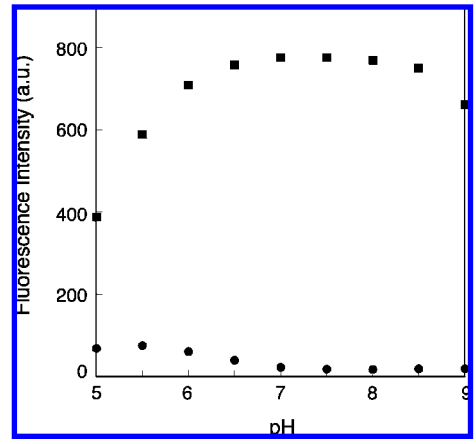

Figure 6. pH-dependent fluorescence profiles of **1**−2Zn(II) and the corresponding ATP binding complex. Measurement conditions: 5 μM **1**−2Zn(II) in the presence (■) or absence (●) of ATP (10 μM) in 5 mM HEPES, 5 mM MES, $\lambda_{ex} = 488$ nm, 25 °C.

fluorescence visualization of intracellular ATP particulate stores in living cells.[14] It has been known that ATP is accumulated within cytoplasmic particulates in high concentration (up to a hundred millimolar) in many types of cells.[15] There is much evidence that ATP stores in neuronal cells serve as the source of extracellular ATP released as a signaling molecule by exocytosis, whereas the role of the ATP store in non-neuronal cells is still controversial.[14,16] Prior to the imaging study, we evaluated the effect of pH change on the fluorescence intensity of **1**−2Zn (II). As shown in Figure 6, significant fluorescence intensity changes were not observed in both cases of **1**−2Zn(II) and the corresponding ATP binding complex of **1**−2Zn(II) in the range from pH 6 to 9. Although the fluorescence intensity of the ATP binding complex was decreased under acidic conditions below pH 6, **1**−2Zn(II) still retained a high sensing ability toward ATP with a large fluorescence enhancement ($F/F_o = 5.7$). This result indicates that the turn-on fluorescence sensing of **1**−2Zn(II) works effectively in the physiological pH conditions. Since **1**−2Zn(II) did not penetrate cell membrane, **1** was modified by acetylation at both hydroxyl groups to increase its lipophilicity. Treatment of **1**−2Zn(II) with acetic anhydride in DMF and subsequent decomplexation of the zinc(II) by EDTA gave the acetylated ligand **4**.

When Jurkat cells, a human T-cell lymphoblast-like cell line, were treated with 10 μM zinc(II) complex of **4** (**4**−2Zn(II)) for 15 min in HBS buffer, a bright fluorescence was observed inside the cells, which appeared particulate and localized in the cytoplasm (Figure 7a). It is clear that the nonfluorescent **4**−2Zn(II) penetrated into the cells and was then hydrolyzed by intracellular esterases to form the fluorescent **1**−2Zn(II). It is to be noted that the fluorescence particles of **1**−2Zn(II) merged well with the fluorescence image obtained by costaining with quinacrine, a widely used probe to locate the ATP store (Figure 7b and 7c).[14,17] This result indicates that **1**−2Zn(II) accumulates in the particulates containing a high concentration of ATP and selectively visualizes them inside the living cells. In the case of the

(14) Yagutkin, G. G.; Mikhailov, A.; Samburski, S. S.; Jalkanen, S. *Mol. Biol. Cell.* **2006**, *17*, 3378.

(15) Sperlágh, B.; Vizi, E. S. *Semin. Neurosci.* **1996**, *18*, 175.

(16) (a) Lazarowski, E. R.; Boucher, R. C.; Harden, T. K. *Mol. Pharmacol.* **2003**, *64*, 785. (b) Bodin, P.; Burnstock, G. *Nuerochem. Res.* **2001**, *26*, 959.

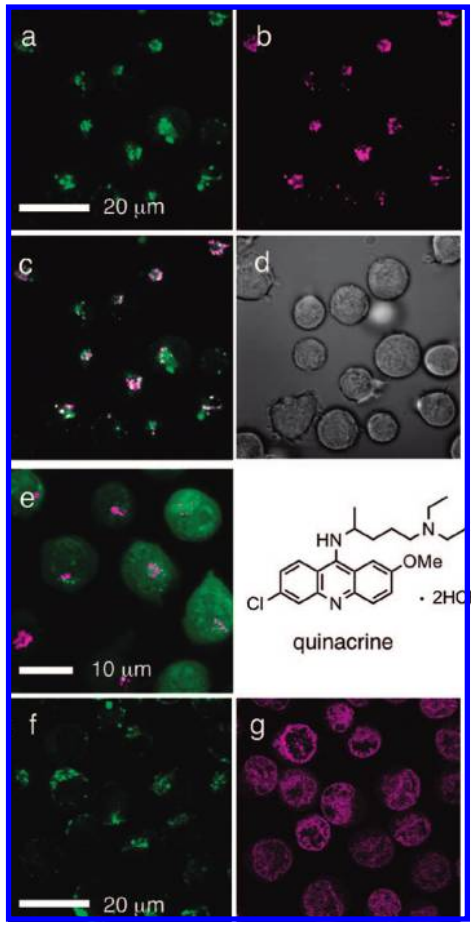

Figure 7. Fluorescence staining of the intracellular ATP stores of Jurkat cells. Each panel (a−d) shows a confocal micrograph obtained at a different fluorescence channel of **1**−2Zn(II) (a) and quinacrine (b), overlay of the two fluorescence images (c), and image of differential interference contrast (DIC) (d). (e) Overlay of the two confocal fluorescence images obtained by staining with ligand **4** and quinacrine. (f and g) Confocal micrograph obtained at a different fluorescence channel of **1**−2Zn(II) (f) and quinacrine (g), respectively, after treatment of 100 μM monensin for 10 min.

staining experiment with ligand **4** in the absence of Zn(II) ions, the fluorescence spread over the cytosol region and did not localize as particles (Figure 7e), suggesting that the Zn(II)/Dpa units of **1**−2Zn(II) are essential for selective staining of ATP stores inside the living cells. When the cells were treated with monensin, a potent *v*-ATPase inhibitor,[17c,18] the fluorescent particles of quinacrine almost disappeared and spread over the cytosol region (Figures 7g and S5b). In contrast, the fluorescent particles indicated by **1**−2Zn(II) did not disappear and remained as the granular pattern (Figures 7f and S5a). This observation is reasonably ascribed to neutralization of acidic vesicular compartments of ATP stores, which induced release of the deprotonated (neutral) quinacrine from the compartment to the cytosol region. In fact, the fluorescent particulates of quinacrine were recovered 20 min along with reacidification of the compartments by washing of the extra cellular solution due to the reversible action of the drug (Figure S5b). These results may suggest that **1**−2Zn(II) is able to visualize the ATP stores regardless of pH change, while staining by the conventional quinacrine is dependent on the pH of the compartment of ATP stores.

In conclusion, we developed the new xanthene-type chemosensor **1**−2Zn(II), which selectively senses nucleoside polyphosphates such as ATP with an off/on fluorescence signal. The turn-on sensing mechanism of **1**−2Zn(II) is based on the recovery of the conjugated xanthene fluorophore from the deconjugated (nonfluorescent) form upon anion binding. Such reformation of the conjugated xanthene triggered by analyte binding or enzymatic reaction has been widely used as a versatile fluorogenic sensing mechanism, as reported in various types of chemical probes.[19,20] We have now successfully introduced this mechanism into anion sensing for the first time by virtue of the unprecedented nucleophilic attack of the zinc-bound water to the xanthene ring. It is expected that the present mechanism is applicable in general as a new design principle for anion chemosensors. The utility of **1**−2Zn(II) as a bioanalytical molecular tool has also been demonstrated by fluorescence imaging of ATP particulate stores in living cells. However, sophisticated chemosensors with a higher selectivity among phosphate species are apparently required for more precise and sensitive analysis of nucleoside polyphosphates and their relevant biological behavior. Our research is now in progress along this line on the basis of the present turn-on fluorescence sensing.

Experimental Section

Synthesis of 1−2Zn(II). 1,8-Bis[(2,2′-dipicolylamino) methyl]-3,6-dipivaloxyxanthone (7). A degassed solution of **5** (600 mg, 1.41 mmol), *N*-bromosuccinimide (NBS) (552 mg, 3.10 mmol), and a catalytic amount of benzoyl peroxide (BPO) in CCl_4 (40 mL) was refluxed for 4 h, during which time a catalytic amount of BPO was added at each 30 min interval. The reaction was monitored by ^{1}H NMR. After cooling to room temperature, the solvent was removed by evaporation and the residue dissolved in AcOEt. The organic layer was washed with saturated $NaHCO_3$ and brine followed by drying over $MgSO_4$. After removal of the solvent in vacuo, the solid was collected by filtration and washed with hexane/*i*-Pr_2O (1:1) to give **6** (532 mg) as a mixture with the corresponding tribromo derivative. The ratio of the dibromo and tribromo derivative was determined by ^{1}H NMR to be ca. 2:1. FAB-MS *m/e* 583 $[M + H]^+$ (dibromo derivative **6**) and 661.0 $[M + H]^+$ (tribromo derivative).

To a cooled (0 °C) solution of 2,2′-dipicolylamine (Dpa) (357 mg, 1.79 mmol) and K_2CO_3 (370 mg) in anhydrous DMF (10 mL) was added **6** (520 mg as a mixture with the tribromo derivative), and the solution was stirred for 1 h at rt. After dilution with H_2O, the mixture was extracted with AcOEt (×2), and the organic layers were washed with H_2O and brine followed by drying over $MgSO_4$. The solvent was removed by evaporation, and the residue was purified by flash column chromatography on silica gel (CH_2Cl_2:MeOH:aqueous NH_3 = 300:10:1 → 200:10:1). The obtained solid was washed with *i*-Pr_2O to give **7** (369 mg, 33% from **5**) as a pale yellow powder.

(17) (a) Pryazhnikov, E.; Khiroug, L. *Glia* **2008**, *56*, 38. (b) Pangrisic, T.; Potokar, M.; Stenovec, M.; Kreft, M.; Fabbretti, E.; Nistri, A.; Pryazhnikov, E.; Khiroug, L.; Giniatullin, R.; Zorec, R. *J. Biol. Chem.* **2007**, *282*, 28749. (c) Bodin, P.; Burnstock, G. *J. Cardiovasc. Pharmacol.* **2001**, *38*, 900. (d) Sorensen, C. E.; Novak, I. *J. Biol. Chem.* **2001**, *276*, 32925. (e) Mitchell, C. H.; Carré, D. A.; McGlinn, A. M.; Stone, R. A.; Civan, M. M. *Proc. Natl. Acad. Sci.* **1998**, *95*, 7174.
(18) Tycko, B.; Keith, C. H.; Maxfield, F. R. *J. Cell Biol.* **1983**, *97*, 1762.
(19) Rotman, B.; Zderic, J. A.; Edelstein, M. *Proc. Natl. Acad. Sci. U.S.A.* **1963**, *50*, 1.
(20) (a) Recent examples of the xanthene-based fluorogenic chemosensors: Kenmoku, S.; Urano, Y.; Kojima, H.; Nagano, T. *J. Am. Chem. Soc.* **2007**, *129*, 7313. (b) Song, F.; Garner, A. L.; Koide, K. *J. Am. Chem. Soc.* **2007**, *129*, 12354. (c) Yang, D.; Wang, H.-L.; Sun, Z.-N.; Chung, N.-W.; Shen, J.-G. *J. Am. Chem. Soc.* **2006**, *128*, 6004. (d) Ko, S.-K.; Yang, Y.-K.; Tae, J.; Shin, I. *J. Am. Chem. Soc.* **2006**, *128*, 14150. (e) Miller, E. W.; Albers, A. E.; Pralle, A.; Isacoff, E. Y.; Chang, C. J. *J. Am. Chem. Soc.* **2005**, *127*, 16652. (f) Maeda, H.; Yamamoto, K.; Nomura, Y.; Kohno, I.; Hafsi, L.; Ueda, N.; Yoshida, S.; Fukuda, M.; Fukuyasu, Y.; Yamauchi, Y.; Itoh, N. *J. Am. Chem. Soc.* **2005**, *127*, 68.

^{1}H NMR (400 MHz, $CDCl_3$) δ 1.38 (18H, s), 3.98 (8H, s), 4.51 (4H, s), 7.07 (2H, d, J = 2.4 Hz), 7.09−7.12 (4H, m), 7.53 (4H, d, J = 7.6 Hz), 7.59 (4H, dt, J = 2.0, 7.6 Hz), 7.83 (2H, d, J = 2.4 Hz), 8.51 (4H, dd, J = 0.8, 4.8 Hz). ^{13}C NMR (100 MHz, $CDCl_3$) δ 27.03, 39.27, 57.29, 60.62, 108.57, 117.73, 118.58, 121.85, 122.41, 136.36, 145.66, 149.12, 154.94, 157.28, 159.53, 176.16, 179.06. FAB-MS *m/e* 819 $[M + H]^+$.

3,6-Dihydroxy-1,8-bis[(2,2′-dipicolylamino)methyl]-9*H*-xanthene (8). To a heated (60 °C) solution of $LiBH_4$ (50 mg, 2.30 mmol) in dry THF (10 mL) was added dropwise a solution of **7** (100 mg, 0.12 mmol) in dry THF (10 mL) over 20 min. The mixture was stirred at 60 °C for 30 min. After cooling to rt, chlorotrimethylsilane (TMSCl) (100 μL) was added, and the mixture was further stirred for 10 min at rt. The reaction was quenched with water, and the resulting mixture was neutralized with aqueous HCl and extracted with CH_2Cl_2 (×2). The organic layers were washed with sat. $NaHCO_3$ and brine followed by drying over Na_2SO_4. The solvent was removed by evaporation to give a colorless solid. The solid was dissolved in 4 N NaOH−MeOH−THF (1:1:2, 8 mL), and the mixture was heated at 60 °C for 4 h. After neutralization with aqueous HCl, the resulting mixture was extracted with CH_2Cl_2 (×3). The organic layers were dried with Na_2SO_4 and concentrated by evaporation. The residue was purified by flash column chromatography on silica gel (CH_2Cl_2:MeOH:NH_3 = 300:10:1 → 200:10:1) to give **8** (48 mg, 62%) as a pale yellow powder. ^{1}H NMR(400 MHz, DMSO-d_6) δ 3.57 (4H, s), 3.72 (10H, s), 6.24 (2H, s), 6.79 (2H, s), 7.21 (4H, t, J = 6.0 Hz), 7.48 (4H, d, J = 8.0 Hz), 7.69 (4H, t, J = 7.6 Hz), 8.46 (4H, d, J = 4.8 Hz). ^{13}C NMR (100 MHz, DMSO-d_6) δ 20.66, 54.92, 59.41, 101.17, 109.35, 111.10, 122.11, 122.40, 136.47, 138.63, 148.81, 151.29, 156.24, 158.87. FAB-MS *m/e* 637 $[M + H]^+$.

1,8-Bis[(2,2′-dipicolylamino)methyl]-6-hydroxy-3*H*-xanthen-3-one (1). To a solution of **1** (69.5 mg, 0.11 mmol) in dry EtOH−CH_2Cl_2 (2:1, 6 mL) was added dropwise a solution of DDQ (29.7 mg, 0.13 mmol) in dry EtOH (4 mL). The mixture was stirred for 10 min at rt. After removal of the solvent by evaporation, the residue was purified by flash column chromatography on silica gel ($CHCl_3$:MeOH:NH_3 = 100:10:1) to give an orange solid. The solid was further purified by precipitation from THF−AcOEt twice to give **1** (58 mg, 83%) as a bright orange powder. ^{1}H NMR(400 MHz, DMSO-d_6) δ 3.79 (8H, s), 3.99 (4H, s), 6.39 (2H, brs), 6.87 (2H, brs), 7.19 (4H, t, J = 6.0 Hz), 7.43 (4H, d, J = 8.0 Hz), 7.65 (4H, t, J = 7.6 Hz), 8.46 (4H, d, J = 4.8 Hz), 8.92 (1H, s). ^{13}C NMR (100 MHz, DMSO-d_6) δ 54.83, 59.43, 122.01, 122.47, 133.07, 136.32, 140.67, 148.78, 158.48. FAB-HRMS *m/e* calcd for $C_{39}H_{35}N_6O_3$ $[M + H]^+$ = 635.277, obsd 635.2765.

1,8-Bis[(2,2′-dipicolylamino)methyl]-6-hydroxy-3*H*-xanthen-3-one 2ZnCl$_2$ Complex (1−2Zn(II)). An aqueous solution of $ZnCl_2$ (100 mM; 831 μL, 0.831 mmol) was added to a solution of **1** (27.8 mg, 0.437 mmol) in distilled MeOH (5 mL), and the mixture was stirred for 30 min at rt. After removal of the solvent by evaporation, the residue was dissolved in distilled water. The solution was filtered through a PTFE filter (pore size, 0.50 μM) and lyophilized. The obtained solid was washed with THF by filtration and dried in vacuo to give **1**−2Zn(II) (30.5 mg, 92%) as a bright orange powder. ^{1}H NMR (400 MHz, DMSO-d_6) δ 3.84 (4H, br), 3.96 (8H, br), 6.10 (2H, br), 6.78 (2H, br), 7.39 (4H, d, J = 3.6 Hz), 7.49 (4H, br), 7.92 (4H, br), 8.72 (4H, br) 11.12(2H, br). FAB-HRMS *m/e* calcd for $C_{39}H_{34}N_6O_3Zn_2Cl_2 \cdot OH$ ($[\mathbf{1}-2Cl + OH]^+$ = 849.0680, obsd 849.0714. Anal. Calcd for $C_{39}H_{34}N_6O_3 \cdot 2ZnCl_2 \cdot 2H_2O$: C, 48.72; H, 4.19; N, 8.74. Found: C, 48.97; H, 3.96; N, 8.77.

3,6-Diacetoxy-9-hydroxy-1,8-bis[(2,2′-dipicolylamino)-methyl]-9*H*-xanthene (4). To a suspension of **1**−2Zn(II) (32.9 mg, 0.035 mmol) in dry DMF (4 mL) was added acetic anhydride (200 μL, 2.13 mmol) and NEt_3 (290 μL, 2.09 mmol). The mixture was stirred for 2 h at rt. After dilution with aqueous EDTA solution (50 mM; 100 mL), the resulting mixture was extracted with $CHCl_3$ (×2). The organic layers were washed with water and dried over Na_2SO_4. After removal of the solvent by evaporation, the residue was purified by HPLC (column;YMC-pack, ODS-A, 250 × 20 mm, mobile phase; CH_3CN (0.1% TFA)/H_2O (0.1% TFA) = 0/100 → 50/50 (linear gradient over 50 min); flow rate, 9.9 mL/min; detection, UV at 220 nm). The fractions were collected and lyophilized to give **4** (10 mg, 40%) as a colorless oil. ^{1}H NMR(400 MHz, DMSO-d_6) δ 2.30 (6H, s), 4.07 (8H, s), 4.15−4.34 (4H, dd, J = 14.0 Hz), 6.20 (1H, s), 6.97 (2H, d, J = 2.4 Hz), 7.28 (2H, d, J = 2H), 7.35 (4H, t, J = 5.2 Hz), 7.49 (4H, d, J = 8.0 Hz), 7.83 (4H, t, J = 7.6 Hz), 8.53 (4H, d, J = 4.8 Hz). FAB-HRMS *m/e* calcd for $C_{43}H_{40}N_6O_6$, obsd 736.2992 ($[M]^+$ = 736.3009).

Fluorescence Measurement. Fluorescence spectra were recorded on a Perkin-Elmer LS55 spectrometer. The fluorescence quantum yield of **1**−2Zn(II) was determined in neutral aqueous solution (50 mM HEPES, 10 mM NaCl, 1 mM $MgCl_2$, pH 7.4) using fluorescein (Invitrogen, F1300) in 0.1 N NaOH as a standard. The titration experiments with the phosphate anion species (Figures 3 and S2, Table 1) were carried out with a solution (3 mL) of **1**−2Zn(II) (1 μM) or **2**−Zn(II) (1 μM) in 50 mM HEPES, 10 mM NaCl, 1 mM $MgCl_2$, pH 7.4 in a quartz cell at 25 °C. The fluorescence emission spectral change (excitation wavelength λ_{ex} = 488 nm) was monitored upon addition of a freshly prepared aqueous solution of the analyte with a microsyringe. Fluorescence titration curves at 523 nm were analyzed with the nonlinear least-squares curve-fitting method to evaluate the apparent binding constant (K_{app}, M^{-1}). Abbreviations of the analytes listed in Table 1 are as follows: ATP = adenosine-5′-triphosphate, ADP = adenosine-5′-diphosphate, AMP = adenosine-5′-monophosphate, GTP = guanosine-5′-triphosphate, CTP = cytidine-5′-triphosphate, UDP = uridine-5′-diphosphate, PPi = pyrophosphoric acid, IP_3 = D-*myo*-inositol-1,3,4-triphosphate, cGMP = guanosine-3′,5′-cyclic monophosphate, cAMP = adenosine-3′,5′-cyclic monophosphate, ADP-Gal = adenosine-5′-diphosphogalactose, UDP-Gal = uridine-5′-diphosphogalactose.

Fluorescent Imaging of ATP Stores in Jurkat Cell. Jurkat cells were cultured in RPMI 1640 supplemented with 10% fetal bovine serum (FBS), penicillin (100 units/mL), and streptomycin (100 μg/mL) at 37 °C under a humidified atmosphere of 5% CO_2 in air. The cells (5×10^5) were collected by centrifugation in a plastic tube and resuspended in HBS buffer (containing 107 mM NaCl, 6 mM KCl, 1.2 mM $MgSO_4$, 2 mM $CaCl_2$, 11.5 mM glucose, 20 mM HEPES, pH 7.4). The staining solution of **4**−2Zn(II) (1.38 mM in DMSO) was prepared by treatment of the ligand **4** with a slight excess (3 equiv) of aqueous $ZnCl_2$ solution in DMSO. The fluorescence staining of the cells was carried out with 10 μM (final concentration) **4**−2Zn(II) for 15 min and then with 4 μM (final concentration) quinacrine for 10 min in HBS buffer. The excess of the staining reagents was removed by centrifugation twice in HBS (500 μL). The cell suspension in HBS (200 μL) was placed into a 35-mm glass-bottomed dish (Iwaki Scitech) and analyzed by a confocal scanning laser microscope (Olympus, FLUOVIEW FV1000). The fluorescence images of **1**−2Zn(II) were obtained by excitation with 515 nm and detection from 530 to 630 nm for **1**−2Zn(II), and those of quinacrine were obtained by excitation with 458 nm and detection from 475 to 500 nm.

Acknowledgment. We thank Prof. Yoshinori Naruta and Dr. Yuichi Shimazaki for the opportunity to perform X-ray crystallographic analysis at their institute (IMCE, Kyushu University).

Supporting Information Available: Synthesis and characterization of **2**−Zn(II), UV and fluorescence titration of the ligand **1** and **2** with $ZnCl_2$, Job's plots between 1−2Zn(II) and ATP, and selected data of the fluorescence visualization of ATP stores in Jurkat cells (PDF); X-ray crystallographic data of **1**−2Zn(II)·4ClO_4^- (CIF). This material is available free of charge via the Internet at http://pubs.acs.org.

JA803262W